*ICIC Express Letters*
*Part B: Applications*
Volume **8**, Number **1**, January **2017**

ICIC International ©2017 ISSN 2185-2766
pp. **159–165**

# AN ACCURATE FRUIT TREE CANOPY RECONSTRUCTION METHOD BASED ON DENSE POINT CLOUD

Sheng Wu[1], Boxiang Xiao[2,3,4,5], Xinyu Guo[2,3,4,5], Weiliang Wen[2,3,4,5] and Chunjiang Zhao[1,2,3,4,5,*]

[1]School of Information Science and Technology
Beijing Forestry University
No. 35, Qinghua East Road, Haidian Dist., Beijing 100083, P. R. China
*Corresponding author: zhaocj@nercita.org.cn

[2]Beijing Research Center for Information Technology in Agriculture
[3]National Engineering Research Center for Information Technology in Agriculture
[4]Beijing Academy of Agriculture and Forestry Science
[5]Beijing Key Lab of Digital Plant
No. 11, Shuguanghuayuan Mid Road, Haidian Dist., Beijing 100097, P. R. China

Received June 2016; accepted September 2016

Abstract. *Tree modeling based on point cloud is a hot issue in computer graphics research; furthermore, accurate three-dimensional canopy structure of fruit tree is an important base for study of functional structure model. We present an efficient canopy reconstruction modeling algorithm for fruit tree based on Laplacian contraction and tree morphology constraints. Firstly, we establish directed graph by using k nearest neighbor connection and Laplacian contraction to improve the computational efficiency; and then, a connecting edge weights model is constructed based on the tree knowledge to break off the error close-loops of directed graph, and a cone projection method is used to smooth splicing in directed graph. Finally, a radius solving approach is proposed to repair small branches by point cloud ring cutting. Point cloud data of different morphology fruit trees is used to evaluate the proposed algorithm; the experimental results show that the canopy structure reconstructed by this algorithm is accurate and robust. The constructed canopy could support the applications both in virtual modeling and experimental simulations.*
**Keywords:** Point cloud density, Canopy reconstruction, Fruit tree, Laplacian contraction, Morphology constraints

1. **Introduction.** In recent years, with the improvement of the accuracy and the scanning range of 3D laser scanner, it is widely used to obtain dense point cloud of large irregular objects such as fruit trees canopy. The canopy structure of fruit tree has an important impact on the distribution light, photosynthetic productivity and physiological state organs in the crown [1-3]. So, modeling 3-D trees is a hot research topic in the field of computer graphics. Modeling 3D fruit trees is a challenging task for several well-known reasons, including complex structure and severe occlusions. In the past decades, many methods have been put forward [4-7]. The method scanning-based [8] is widely studied because of its high precision; some of the famous methods include Laplacian smoothing [9,10], directed graph construction [11,12], space colonization [13], global knowledge constraint [14], data driven [15] and so on. However, these methods are not robust enough for dense points cloud and complex branches.

In this paper, we present a novel algorithm for extracting the curve skeletons of fruit tree models to solve the reconstruction accuracy problems as illustrated in Figure 1. The experimental results show that our method is accurate and robust for different fruit trees morphology point cloud.

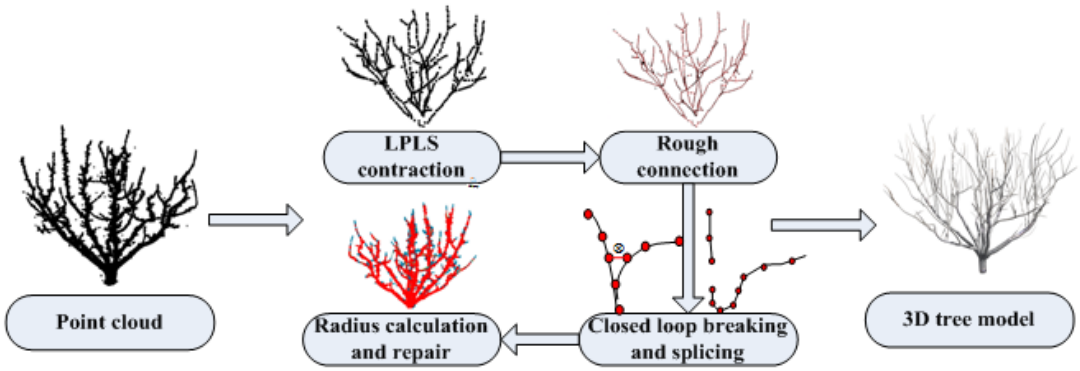


FIGURE 1. The algorithm flow chart

(a) (b) (c)

FIGURE 2. Point cloud scanning, (a) the entity of pear tree, (b) the scanning point cloud, and (c) the key points of contraction by 4 iterations

2. **Point Cloud Scanning.** We use FARO Laser Scanner Focus$^{3D}$ to obtain the point cloud data of fruit trees in leaf fall period. In order to obtain a higher precision, each tree was scanned vertically by 90 degrees, a total of four stacks, the scanning scene and the scanning point cloud effect are shown in Figure 2. In the case of decade raw pear tree, the number of point clouds is about 550,000 after isolated point denoise.

3. **The Algorithm.**

3.1. **Point cloud contraction.** The geometric contraction of the point cloud is implemented on the basis of implicit Laplacian smoothing [9]. In order to improve the efficiency of the algorithm, the point cloud curvature sampling algorithm is used [16], the experience has shown that the data is still valid at 10% ratio sample, the point cloud data is stored in the matrix $P$. As stated in [9], a planar Delaunay triangulation of these points can be constructed easily, and then a Laplacian matrix $L$ is constructed with cotangent weights. The contraction is computed by iteratively solving the linear system:

$$\begin{bmatrix} W_L^t L^t \\ W_H^t \end{bmatrix} P^{t+1} = \begin{bmatrix} 0 \\ W_H^t P^t \end{bmatrix} \tag{1}$$

where $L$ is an $n \times n$ Laplacian matrix with cotangent weights, $P$ is the contracting point cloud, $W_L$ and $W_H$ are the diagonal weight matrices balancing the contraction and attraction forces. In general, the point clouds achieve their convergence within a small number of iterations (Figure 2(c)).

3.2. **Rough connection.** By the previous section method, the point cloud becomes a skeletal shape; however, the contraction nodes are isolated. So we first construct an

incomplete graph on $G$ by constructing node $k$ nearest neighbor, and introduce neighbor distance to reduce the noise edges:

$$d = \frac{2}{n(k-1)} \sum_{i=1}^{n} \sum_{j=1}^{k-1} d_{ij} \tag{2}$$

If the distance between the node and $k$ neighbor nodes is greater than $d$, the adjacent edge is not connected, usually $k = 3$. It is obvious that, if the $k \geq 3$, there are a lot of error triangle closed loops in the incomplete graph (Figure 3). For the left of Figure 3, the noise edge is removed if the side edge corresponding vertical angle is greater than 90 degrees. For the right of Figure 3, the noise edge is removed if the edge has the least neighbor points (In Figure 3 right, the number of neighbor points of edge $\overrightarrow{pp_1}$, $\overrightarrow{pp_2}$, $\overrightarrow{p_1p_2}$ is 6, 5, 2. So the edge $\overrightarrow{p_1p_2}$ is removed). After the implementation for every node, we obtain a two-way connected tree that looks like the skeleton but has some noise edges (Figure 4).

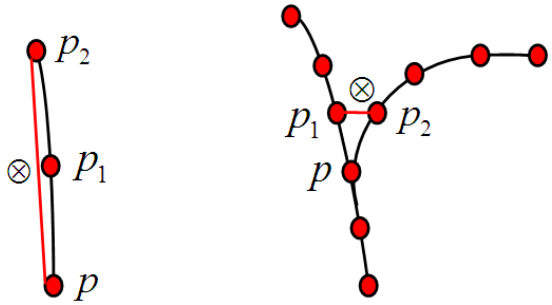


FIGURE 3. The error triangle closed loop

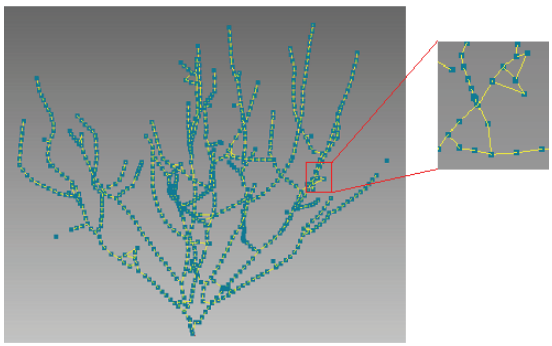

FIGURE 4. The $k$ nearest neighbor connected tree

3.3. **Closed loop breaking.** According to the tree structure knowledge, there is no closed loop in the directed graph. So, we present a method by calculating fracture weights of the directed edges based on the tree knowledge to break off the error close-loops of connected graph. In the tree structure, the nearest neighbor nodes have two principles (coplanar and growth isotropic); therefore, we built edge connectivity weight solution formula:

$$W = W_s * W_c \tag{3}$$

where $W_s$ is coplanar weight, $W_c$ is growth isotropic weight, the minimum weight of the edge is removed. For coplanar principle (Figure 5(a)), we use the least square method to fit the closed loop [17], namely, to solve the equation:

$$ax + by + cz + d = 0, \quad e = \sum_{i=1}^{n} d_i^2 \to \min, \quad W_s = 1/d_i + 1/d_{i+1} \tag{4}$$

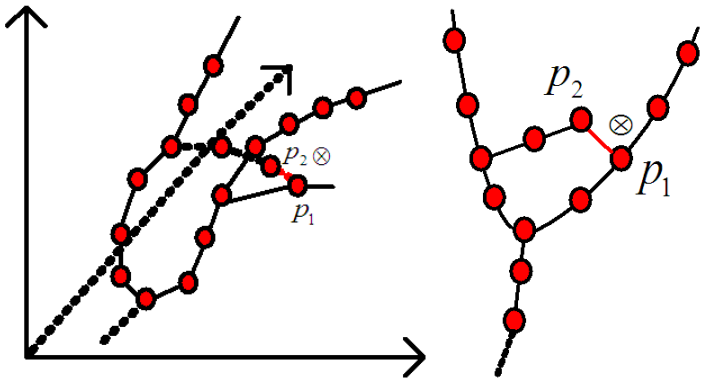


(a) (b)

FIGURE 5. Principle of tree growth, (a) the coplanar principle and (b) the growth isotropic principle

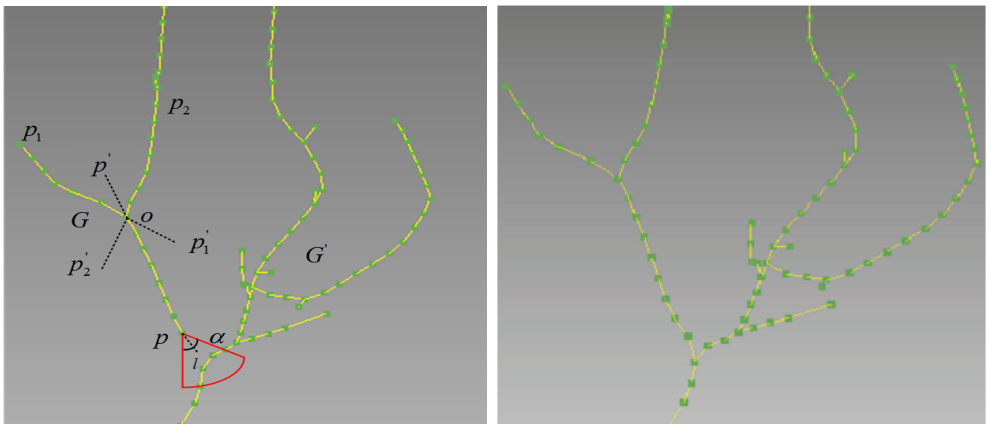


(a) (b)

FIGURE 6. Directed graph splicing, (a) vertebral body mapping, (b) results splicing

For growth isotropic principle (Figure 5(b)), the case has been described in Section 3.1, and is also applicable for the multi point closed loop, with the edge of the angle of more than 150 degrees as the edge of the convergence constraint, so the growth isotropic weight of the edge: $W_c = t$, which is the number of nodes on adjacent edge.

3.4. **Directed graph splicing.** The directed graph is incomplete connected due to lack data (Figure 6(a)). We are inspired by [18], a cone is established in tangent direction of directed graph, we search for the best connection points within the cone range, and then, the connection points are connected by B-Spline fitting.

3.4.1. *The main branch of directed graph.* First of all, we find all single adjacent node of the directed graph, then the largest growth direction angle of each single adjacent node is calculated, and finally, we determined that the access point is the smallest growth angle based on the principle of the branches grow upward. So, the main branch is the connecting edge from the access node to the nearest branch node.

3.4.2. *Directed graph splicing.* We construct a cone in the separation nodes of directed graph. The vertex of cone is the access point $p$, the axis of cone is the main branches tangent and cone angle is $\alpha$ (45 degrees), then, in the cone range we search for the best connection point which is nearest to the tangent distance, and its radius is thicker than

the access point. Finally, B-Spline fitting is established between the access node and the main branch node to achieve the smooth splicing of the separate graph (Figure 6(b)).

3.5. **Small branch repairing based on branch radius.** After the above algorithm, we get a complete directed tree. However, the Laplacian algorithm is not sensitive to small branches. We find the missing small branches point cloud data can be found by ring cutting the directed tree on the basis of the original point cloud. In order to obtain accurate ring cutting operation, firstly we plane ring cut the original point cloud along the edge of the directed tree, and then, the radius is solved by the least square circle fitting the points on the plane. The density-based spatial clustering algorithm [19] is used on missing the points cloud data, and we obtain new nodes, which are connected to the directed tree in accordance with the above algorithm. Thus, the small branches were repaired to the directed tree (Figure 7).

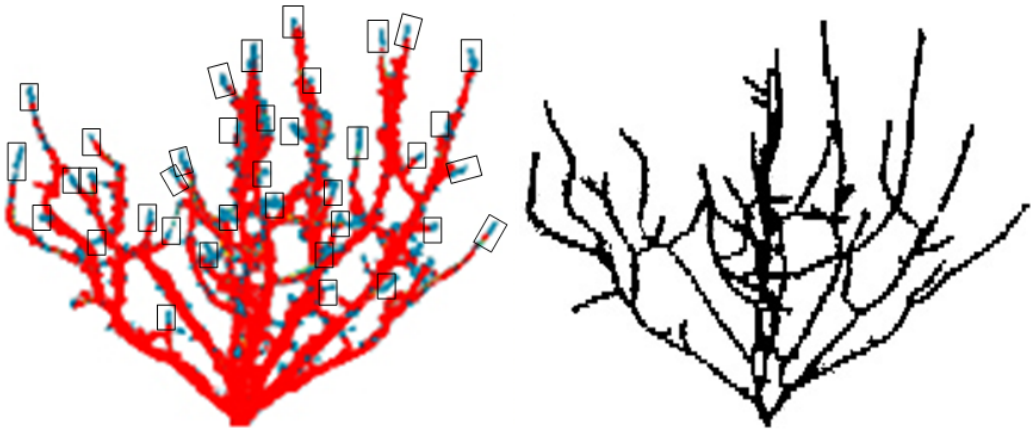

(a) (b)

FIGURE 7. Branch repairing based on radius: (a) the point clouds in each rectangle are missing small branches, and (b) repaired directed connected tree

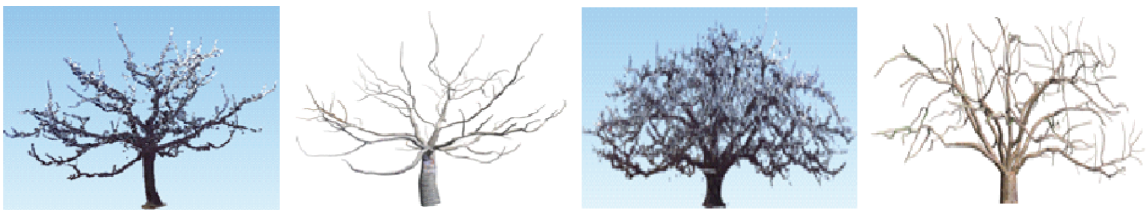

(a) (b) (c) (d)

FIGURE 8. Reconstruction result visualization, (a) and (c) original point cloud of apple and pear trees, (b) and (d) corresponding reconstruction results

4. **Result.** The whole fruit tree canopy is completed based on our method, and tree modeling process generally takes less than 10 minutes on a standard PC with 2G CPU. The reliability of the method is validated by some different fruit tree point clouds including apple, pear, citrus trees, etc. The results demonstrate that our algorithm is accurate and robust for different fruit trees morphology point cloud, 3-D fruit tree visualizations as shown in Figure 8. We compare our method with the work in [10]; the results show that our method can reconstruct smaller branches, have better smoothness and more precise branching structure, as shown in Figure 9.

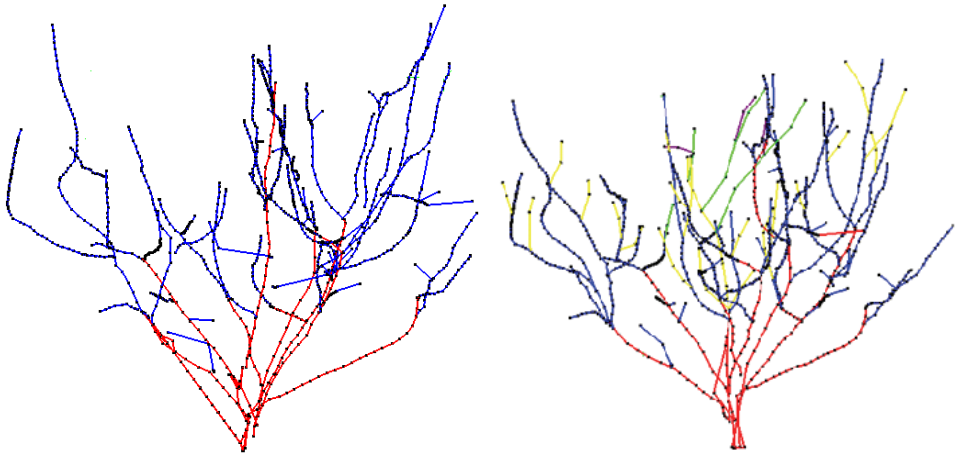

(a) (b)

FIGURE 9. (a) 3-D tree skeleton obtained by the method in [10], and (b) 3-D tree skeleton using our method

5. **Conclusions.** In this paper, we present a novel algorithm for extracting the curve skeletons of fruit tree models to solve the reconstruction accuracy problems. The experimental results show that the 3-D fruit trees using our method are accurate and robust for different fruit trees morphology point cloud. The accuracy of the reconstructed model can meet the needs of the virtual experiment of the agricultural personnel, and our method provides an efficient data acquisition means of canopy structure for the research of the functional structure model of fruit trees. However, our method has low accuracy on the point cloud tree with leaf. In the future, we will study the leaf point clouds segmentation method to overcome this problem.

**Acknowledgements.** This work was supported by the National High Technologies Research and Development Program of China (Grant No. 2013AA102405), by Beijing Municipal Natural Science Foundation (Grant No. 4162028), by National Natural Science Foundation of China (Grant No. 61300079).

## REFERENCES

[1] C. Werner, R. J. Ryel, M. J. Correia et al., Structural and functional variability within the canopy and its relevance for carbon gain and stress avoidance, *Acta Oecologica – International Journal of Ecology*, vol.22, pp.129-138, 2001.

[2] W. Yan, F. Chonghui, J. Daowei et al., Comparison on crown characteristics and fruit quality of different tree canopy shapes, *Acta Agriculturae Boreali-Occidentalis Sinica*, vol.20, no.12, pp.93-97, 2011.

[3] Z. Gao, C. Zhao, J. Cheng et al., Tree structure and 3-D distribution of radiation in canopy of apple trees with different canopy structures in China, *Chinese Journal of Eco-Agriculture*, vol.20, no.1, pp.63-68, 2012.

[4] Z. Cheng, X. Zhang and B. Chen, Simple reconstruction of tree branches from a single range image, *Journal of Computer Science and Technology*, vol.22, no.6, pp.846-858, 2007.

[5] M. Dai, X. Zhang and H. Li, Tree reconstruction based on range image with strong noise, *Chinese Journal of Stereology and Image Analysis*, vol.15, no.2, pp.109-114, 2010.

[6] B. Lintermann and Q. Deussen, Interactive modeling of plants, *IEEE Computer Graphics and Application*, vol.19, no.1, pp.56-65, 1999.

[7] R. Mech and P. Prusinkiewicz, Visual models of plants interacting with their environment, *Proc. of SIGGRAPH'96*, pp.397-410, 1996.

[8] T. Dornbusch, S. Lorrain, D. Kuznetsov and C. Fankhauser, Measuring the diurnal pattern of leaf hyponasty and growth in Arabidopsis – A novel phenotyping approach using laser scanning, *Functional Plant Biology*, vol.39, no.11, pp.860-869, 2012.

[9] J. J. Cao, A. Tagliasacchi, M. Olson, H. Zhang and Z. X. Su, Point cloud skeletons via Laplacian-based contraction, *Proc. of the International Conference on Shape Modeling and Applications*, 2010.
[10] Z. Su, Y. Zhao, C. Zhao et al., Skeleton extraction for tree models, *Mathematical and Computer Modelling*, vol.54, pp.1115-1120, 2011.
[11] Y. Livny, F. Yan, M. Olson et al., Automatic reconstruction of tree skeletal structures from point clouds, *ACM Trans. Graphics*, vol.29, no.6, pp.81-95, 2010.
[12] A. Bucksch and R. Lindenbergh, CAMPINO – A skeletonization method for point cloud processing, *ISPRS Journal of Photogrammetry & Remote Sensing*, no.63, pp.115-127, 2008.
[13] A. Runions, B. Lane and P. Prusinkiewicz, Modeling trees with a space colonization algorithm, *Eurographics Workshop on Natural Phenomena*, pp.63-70, 2007.
[14] Z. Wang, L. Zhang, T. Fang, X. Tong, P. T. Mathiopoulos et al., A local structure and direction-aware optimization approach for three-dimensional tree modeling, *IEEE Trans. Geoscience and Remote Sensing*, no.4, pp.1-9, 2016.
[15] X. Zhang, H. Li, M. Dai, W. Ma and L. Quan, Data-driven synthetic modeling of trees, *IEEE Trans. Visualization and Computer Graphics*, no.9, pp.1214-1226, 2014.
[16] E. Saux and M. Daniel, Data reduction of polygonal curves using B-splines, *Computer-Aided Design*, vol.31, pp.507-515, 1999.
[17] O. Sorkine and D. Cohen-Or, Least-squares meshes, *Proc. of the International Conference on Shape Modeling and Applications*, 2004.
[18] H. Xu, N. Gossett and B. Chen, Knowledge and heuristic-based modeling of laser-scanned trees, *ACM Trans. Graphics*, vol.26, no.4, pp.377-388, 2007.
[19] Q. Liu, M. Deng, Y. Shi and J. Wang, A density-based spatial clustering algorithm considering both spatial proximity and attribute similarity, *Computers & Geosciences*, vol.46, no.3, pp.296-309, 2012.